Hindawi
Geofluids
Volume 2023, Article ID 8851149, 10 pages
https://doi.org/10.1155/2023/8851149

Research Article

Stress Sensitivity of Proppant-Containing Fractures and Its Influence on Gas Well Productivity

Hao Chen,[1,2] **Jianfei Wei**,[1] **Hanlie Cheng**,[1] **Qiang Qin**,[1] **Ying Chen**,[3] **and Linqiang Zhang**[4]

[1]*COSL-EXPRO Testing Services (Tianjin) Co., Ltd., Tianjin 300457, China*
[2]*Unconventional Oil and Natural Gas Institute, China University of Petroleum, Beijing 102249, China*
[3]*Engineering Company, Offshore Oil Engineering Co., Ltd., Tianjin 300451, China*
[4]*China United Coalbed Methane Co., Ltd., Beijing 100011, China*

Correspondence should be addressed to Hanlie Cheng; chenghl@cosl-expro.com

Received 8 December 2022; Revised 21 April 2023; Accepted 26 April 2023; Published 4 May 2023

Academic Editor: Bao Jia

Formation pressure gradually decreases with fracturing fluid flowback and gas production. Due to the stress sensitivity of the fractures, the permeability of the artificial fractures after fracturing becomes lower, which significantly affects gas well productivity. This paper focuses on two questions: (1) the stress sensitivity of proppant-containing fractures with different roughness and (2) tight gas well productivity considering stress sensitivity. Two types of artificial fracture samples, smooth and rough, are prepared and filled with different proppant concentrations. Then, the changing confining pressure method is used to quantify sample stress sensitivity. On this basis, the productivity equation for the fractured well with finite conductivity that considers fracture and matrix stress sensitivity is derived, and the influence of stress sensitivity on productivity is discussed. The results show that proppant concentration and fracture surface roughness will significantly affect fracture permeability and stress sensitivity; with increasing proppant concentration, fracture permeability increases, stress sensitivity decreases, and well productivity increases; under the same proppant concentration, the stress sensitivity is lower and the gas production is higher for smooth fracture; and when the artificial fracture changes from no proppant to proppant, the productivity of the fracturing well is improved the most.

1. Introduction

Since global oil and gas consumption grows continuously, conventional oil and gas development alone cannot meet social needs [1]. Therefore, unconventional oil and gas reservoirs, which cannot be developed conventionally, are receiving more and more attention [2, 3]. In China, unconventional oil and gas resources are widely distributed in Sichuan, Songliao, Ordos Junggar, and other basins, offering considerable development potential and broad prospects [4–7]. However, unconventional reservoirs have extremely low porosity and permeability, which requires massive hydraulic fracturing for effective development [8, 9]. During hydraulic fracturing, artificial fractures are formed as large-scale fracturing fluid enters the formation. Oil and gas well production is strongly affected by these fractures since they are the main channels for reservoir fluid to enter the wellbore after fracturing [10]. With the fracturing fluid flowback and well production, the formation pressure gradually decreases, and the effective stress of the reservoir increases. Due to the stress sensitivity of fractures and reservoir matrix, permeability and fracture conductivity are drastically reduced, resulting in irreversible permeability loss and seriously affecting well productivity [11, 12].

Many researchers have studied reservoir stress sensitivity and oil and gas well productivity, establishing power law, and exponential and polynomial relationships between permeability and stress sensitivity [13–16]. Zhang et al. investigated the influencing factors and control mechanisms of shale stress sensitivity through permeability testing, rock

physical property analysis, and the dual pore medium stress sensitivity model [17, 18]. Rahman and Rahman investigated the interaction between induced and preexisting fractures in naturally fractured reservoirs by a numerical model using finite element analysis [19]. Sun et al. and Liu et al. studied volcanic rocks with different pore types and concluded that fractured volcanic gas reservoir rocks have strong stress-sensitive characteristics [20, 21]. Dong et al. examined the porosity and permeability of shale and sandstone, and the results showed that shale has stronger stress sensitivity than sandstone [22]. Xiao et al. studied the stress sensitivity of coal permeability and indicated that the coal shows significant anisotropic permeability and stress sensitivity due to the complex heterogeneity of the natural fracture system [23]. Yang et al. investigated the stress sensitivity of naturally fractured shale, and the results showed that the permeability evolution is consistent with the fracture aperture change during loading [24]. The above studies are focused on reservoir matrix and natural fractures, and there are fewer studies on artificial fracture permeability stress sensitivity.

Rock plate conductivity experiments are the primary method for studying the effects of closure pressure, proppant concentration, and proppant embedding on the permeability of artificial fractures [25–28]. Shaibu et al. conducted fracture conductivity experiments on saw-cut shale core, and the results showed that the main driver of fracture conductivity was induced fractures. However, permeability data were not obtained for this study, and large-scale cores could not be tested by a conventional permeameter [29] However, the method has several drawbacks, including experimental complexity, large sample size, and preparation difficulties. Therefore, developing a more straightforward experimental method for studying artificial fractures is necessary. Wuguang et al. studied the effect of proppant on stress sensitivity by splitting shale cores and filling the fractures with proppant. This study concluded that proppant filling can effectively enhance the permeability of artificial fractures and reduce stress sensitivity, but this study did not quantify the proppant concentration [10]. Dong et al. and Lei et al. conducted experimental and theoretical research to investigate the effects of stress on fracture width and particle plugging in porous media. The study found that high stress causes increased pore blockage, and larger pores are less likely to experience particle plugging. Closure pressure reduction increases fracture width, as it decreases the contact force between fractured surfaces [30, 31]. Chen et al. used the Brazilian splitting method to create rough fractures and quantified the effect of proppant concentration on the stress sensitivity of artificial fractures by changing gas flow pressure and confining pressure, respectively. It concluded that the stress sensitivity of fractures obtained by the above two methods is not much different at low proppant concentrations, and the test methods significantly affect stress sensitivity at high proppant concentrations [32]. Nevertheless, it did not study the effect of fracture roughness on stress sensitivity.

The effect of stress sensitivity on production has been studied in depth by many scholars. Bo et al. derived a production prediction method considering stress sensitivity and threshold pressure gradient based on the dual-porosity theory model, and the results show that two parameters must be considered in tight gas reservoirs [33]. Jiang et al. established a coupled matrix-fracture fluid flow model and investigated different stress-sensitive effects in different subsystems. This study concluded that the influence of stress sensitivity in fractures depends on the properties and location of the fractures [34]. Xinli conducted stress sensitivity experiments on sandstone containing microfractures and further investigated its effect on productivity, which indicated that the stress sensitivity of sandstone containing microfractures had little effect on oil production [35]. Liu et al. studied the stress sensitivity of low permeability reservoirs and its impact on oil and gas development through experiments and theoretical derivations and concluded that the lower the permeability and the faster the loading rate, the higher the permanent damage rate; the stronger the heterogeneity, the greater the productivity is affected by stress sensitivity [36]. The above studies of well production either did not conduct stress sensitivity experiments or only considered matrix stress sensitivity.

In this research, core-scale smooth and rough artificial fracture samples were prepared by wire cutting and splitting, respectively. Then, the samples were filled with different proppant concentrations. The influence of proppant concentration and fracture surface roughness on permeability and stress sensitivity was investigated by a conventional gas-measured permeability apparatus. Furthermore, the productivity equation of fractured gas wells considering matrix and artificial fracture stress sensitivity is derived to study the effect of stress sensitivity on well productivity. The objective of this study is to introduce a practical approach to conducting core-scale fracturing experiments, examine the stress sensitivity of fractures containing proppant, and evaluate the production capacity of gas wells in various types of fractures. This study helps to understand the flow of geofluids in fractures after fracturing and provides a basis for optimizing hydraulic fracture design and fracture fluid flowback procedures.

2. Experimental Method

2.1. Sample Preparation. In this study, samples were collected from the sedimentary pyroclastic rock of the Lower Cretaceous Yingcheng Formation in Songliao Basin, northeastern China. The logging data indicates that the porosity of this formation is 10.78% and the permeability is $0.19 \times 10^{-3}\ \mu m^2$. In order to study the fracture surface with different roughness, wire cutting and splitting methods were used to make artificial fractures. Artificial fractures with smooth surfaces can be obtained by wire cutting, as shown in Figure 1(a), and artificial fractures with rough surfaces can be obtained by splitting, as shown in Figure 1(b).

The proppant used in this experiment was ceramic granules with a mesh size of 40/70 and an apparent density of $1570\ kg/m^3$. According to the designed proppant concentration, the theoretical fracture width and proppant mass were calculated. The cores were prepped with theoretical fracture widths, the sample side was taped tightly, and then one side

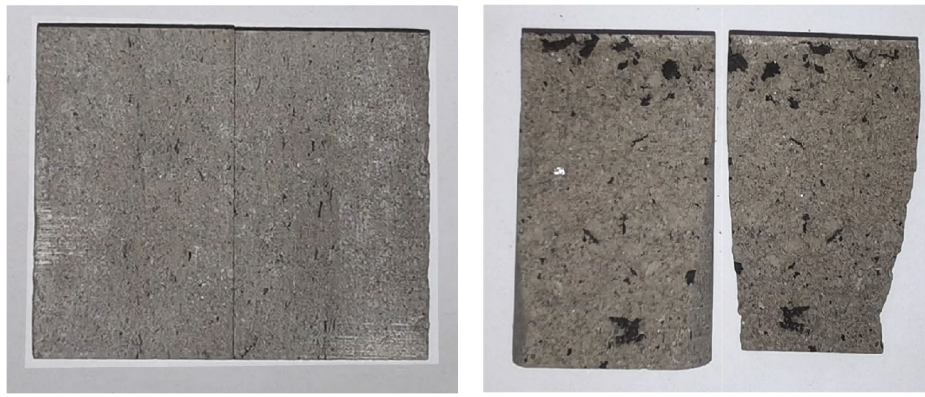

(a) (b)

Figure 1: Experimental materials: (a) smooth fracture sample; (b) rough fracture sample.

end face was sealed with gauze. After that, the proppant was placed in fracture, and another side end face was sealed with gauze. At last, the actual width and proppant concentration were calculated by the actual proppant addition mass by the following formulas:

$$c_p = \frac{m_{\text{prop}}}{dL}, \tag{1}$$

$$w = \frac{c_p}{\rho_{\text{prop}}}, \tag{2}$$

where c_p is proppant concentration, kg/m^2; m_{prop} is proppant mass, kg; d and L are the diameter and length of the sample, m; w is fracture width, m; and ρ_{prop} is proppant apparent density, kg/m^3.

This experiment consisted of 4 smooth fracture samples and 2 rough fracture samples, with 1 nonfractured matrix sample used as a comparison. The basic parameters of the samples are shown in Table 1.

2.2. Experimental Method and Procedure. In this study, a gas-measured permeability apparatus was employed to investigate the stress sensitivity of artificial fracture. The test is conducted by changing confining pressure, and the test fluid is nitrogen with 99.9% purity. Following the requirements of SY/T 5358-2010 Formation damage evaluation by flow test, the specific experimental procedure is as follows:

(1) *Basic Parameter Testing*. Dry the cores and measure the length, diameter, and mass of the samples

(2) *Artificial Fracture Preparing*. Smooth surfaces can be obtained by wire cutting, and rough fractures are prepared by the splitting method. Dry and weigh the samples again

(3) *Proppant Filling*. Fill the fractures with proppant as designed and then calculate the proppant concentration based on the actual mass

(4) *Permeability Testing*. The permeability tests are performed with a constant gas flow pressure of 0.05 MPa and confining pressure of 2, 5, 9, 15, 20, 25, and 30 MPa. During the test, each designed confining pressure is maintained for more than 30 min, waiting for the flow to stabilize before metering begins. The following equation can calculate the gas permeability of the samples:

$$k_g = \frac{2q_0p_0\mu L}{A\left(p_1^2 - p_2^2\right)}, \tag{3}$$

where k_g is gas permeability, m^2; q_0 is gas flow rate, m^3/s; μ is nitrogen viscosity, Pa·s; A is the cross-sectional area of the sample, m^2; and p_1 and p_2 are the pressures at the inlet and outlet of the sample, respectively, Pa.

The effective stress of the sample was calculated by Terzaghi's effective stress equation:

$$p_e = p_c - p_f, \tag{4}$$

where p_e is effective stress, MPa; p_c is confining pressure, MPa; and p_f is gas flow pressure, MPa.

3. Experimental Results and Discussions

3.1. Permeability Variation Rules with Effective Stress. The permeability test results of the samples are shown in Table 2. By normalizing the permeability based on the permeability at effective stress of 2 MPa, the variation of normalized permeability with effective stress can be obtained (Figure 2). As can be seen in the figure, the permeability of the sample gradually decreases with increasing effective stress. As effective stress increases, the reduction rate of permeability decreases.

When effective stress was increased from 2 MPa to 15 MPa, samples 1#-7# lost 74.47%, 36.37%, 22.48%, 12.18%, 84.18%, 66.52%, and 55.61% of their permeability. Comparatively, only 17.28%, 22.50%, 22.29%, 9.67%, 14.40%, 26.67%, and 21.93% of permeability were lost in 15-30 MPa loading intervals for samples 1#-7#. This is because the initial proppant is loosely arranged and more easily compressed, leading to a reduction in fracture width

Table 1: Basic parameters of the samples.

Fracture type	Sample number	Length (mm)	Diameter (mm)	Fracture width (mm)	Proppant concentration (kg/m^2)
Smooth	1#	50.02	24.36	0	0
	2#	48.24	24.34	0.36	0.57
	3#	49.75	24.36	0.66	1.04
	4	47.36	24.24	1.11	1.75
Rough	5#	49.68	24.32	0	0
	6#	48.97	24.34	0.34	0.54
Nonfractured	7#	49.37	24.36	—	—

Table 2: Permeability test results of samples.

p_e (MPa)	Permeability ($\times 10^{-3}$ μm^2)						
	Smooth fracture				Rough fracture		Matrix
	1#	2#	3#	4#	5#	6#	7#
2	241.42	1921.01	2418.00	3350.00	263.21	1413.00	0.187
5	180.62	1737.92	2290.00	3158.00	166.41	1181.25	0.165
9	148.06	1586.46	2032.00	3053.00	94.10	756.78	0.122
15	61.63	1222.27	1874.54	2942.00	41.63	473.13	0.083
20	35.41	999.94	1660.93	2805.00	12.00	283.69	0.062
25	23.04	876.56	1484.89	2681.00	6.20	201.61	0.051
30	19.91	790.13	1335.55	2618.00	3.74	96.26	0.042

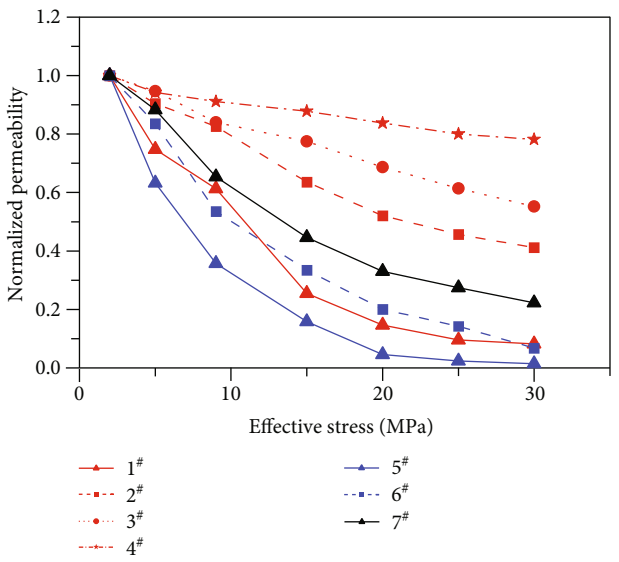

Figure 2: The relationship between normalized permeability and effective stress.

and a decrease in permeability. As the effective stress increases, the proppant arrangement becomes tighter and more difficult to compress, the fracture structure does not easily change, and the permeability decreases slower.

This result is similar in trend to those researches of Wuguang et al. and Chen et al. on shale [10, 32], but with a more significant permeability loss in the rough fracture samples of the same proppant concentration compared to Chen et al. There are two possible reasons for this: One is that the sedimentary pyroclastic rock used in this experiment has a relatively low hardness compared to shale, which is more likely to deform when the effective stress is changed. Another is that laminae are developed in shale, and fractures are easily generated along the surface of laminates when the shale is split. The fracture surfaces of shale are smoother, and the proppant distribution will be relatively uniform, reducing the likelihood of permeability reduction caused by partial low proppant concentration.

3.2. Effect of Proppant Concentration on Permeability and Stress Sensitivity. The permeability is normalized based on the fracture samples without proppant, and the normalized permeability versus proppant concentration is represented in Figure 3. The normalized permeability is defined as follows:

$$k_{Nc_p} = \frac{k_i}{k_{i,c_p=0}}, \tag{5}$$

where k_{Nc_p} is normalized permeability, dimensionless; k_i is permeability under i effective pressure, m^2; and $k_{i,c_p} = 0$ is permeability of fracture samples without proppant under i effective pressure, m^2.

The figure shows that with an increase in the proppant concentration, whether in smooth or rough fracture samples, the permeability increases significantly under each effective stress. It shows that the higher the effective stress, the greater the normalized permeability. Taking the smooth fracture samples as an example, when the effective stress is 2 MPa, the permeability of the samples with sand concentrations of 0.57, 1.04, and 1.75 kg/m^2 is 7.96, 10.02, and 13.88

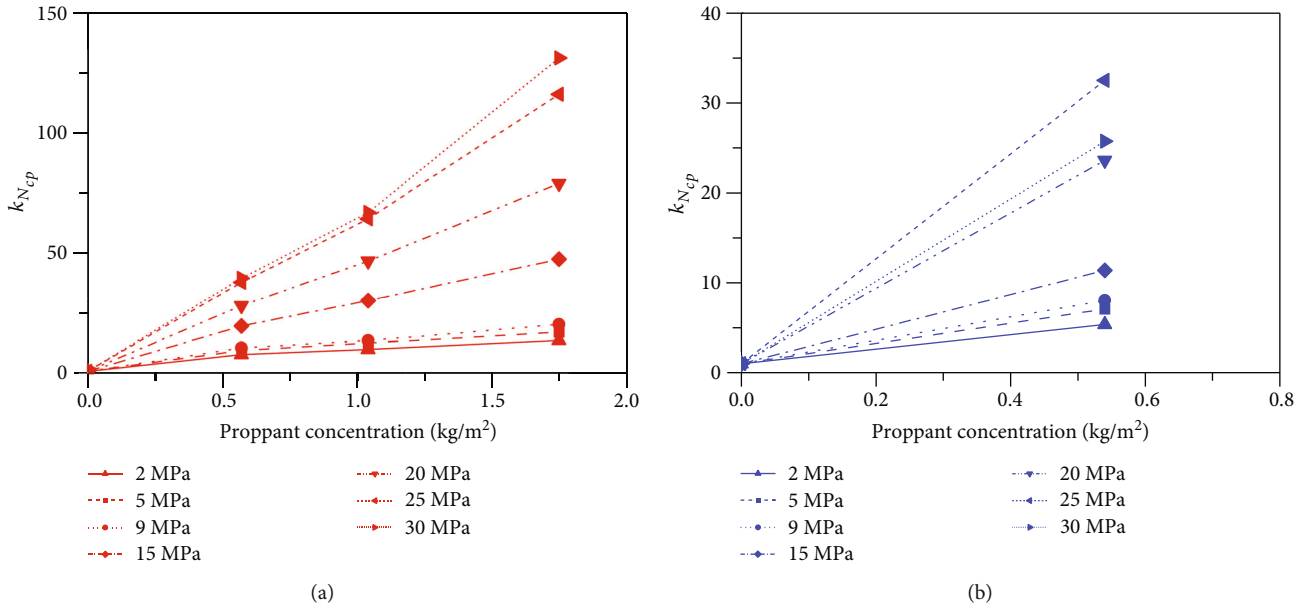

FIGURE 3: The relationship between normalized permeability (k_{Nc_p}) and proppant concentration: (a) smooth fracture; (b) rough fracture.

times greater than that of the sample without proppant. Comparatively, the values at 30 MPa are 39.69, 67.08, and 131.49 times. This is because as the effective stress increases, the arrangement of the proppant becomes tighter and tighter, the support capacity gradually increases, and the permeability increase multiplier becomes larger accordingly.

Based on Figure 3, a segmented linear fit is performed to determine each stage's slope separately. The slope is defined as the proppant efficiency, as shown in the following equation:

$$E_{\text{prop}} = \frac{\Delta k_{Nc_p}}{\Delta c_p}, \tag{6}$$

where E_{prop} is proppant efficiency, m^2/kg; Δc_p is the proppant concentration change in a certain stage, kg/m^2; and Δk_{Ncp} is normalized permeability change in the corresponding stage, dimensionless. The physical meaning of proppant efficiency is the multiple of the increase in permeability per unit proppant concentration at this stage.

As shown in the proppant efficiency statistical graph (Figure 4), the proppant efficiency is enhanced with increased effective stress in the same proppant concentration interval. Taking the proppant concentration interval of 0-0.57 kg/m^2 as an example, the proppant efficiency of this interval increased from 13.96 m^2/kg to 69.62 m^2/kg when the effective stress increased from 2 MPa to 30 MPa.

The proppant efficiency decreases with increasing proppant concentration under the same effective pressure. For the same effective stress of 2 MPa, the proppant efficiency was 13.96, 2.68, and 1.95 m^2/kg for proppant concentration intervals of 0-0.57, 0.57-1.04, and 1.04-1.75 kg/m^2, respectively. It indicates that the lower the proppant concentration, the more effective it is to increase the proppant concentration in improving permeability.

During hydraulic fracturing, in addition to increasing the proppant amount, a proper proppant-adding method should be used to allow proppant to reach fractures with low proppant concentrations, such as the deep portion of the main fracture and the secondary fractures, as much as possible. Thus, the average proppant concentration of fractures is enhanced, and the permeability of fractures is greatly improved. The proppant efficiency for rough fractures is lower at 30 MPa than 25 MPa. This may be caused by the proppant starting embedding in the fracture surface during the effective stress interval between 25 and 30 MPa.

An exponential fitting is performed on the effective stress and permeability to obtain the sample's stress sensitivity coefficient. The fitting equation is given by

$$k = k_0 e^{-bp_e}, \tag{7}$$

where k and k_0 are permeability and initial permeability, respectively, $10^{-3}\,\mu$m^2, and b is the stress sensitivity coefficient, MPa^{-1}.

Since the permeability of the artificial fracture sample is much larger than the matrix permeability, the matrix permeability can be ignored for the artificial fracture sample. Therefore, the permeability of the sample in the experiment is regarded as the fracture permeability, and the stress sensitivity coefficient of the sample is considered to be the stress sensitivity coefficient of artificial fracture.

Figure 5 shows the stress sensitivity coefficient of each sample. In this experiment, the smooth fracture sample without proppant and the rough fracture samples reveal strong stress sensitivity. The matrix sample presents medium stress sensitivity, while the smooth fracture with proppant shows moderately weak to weak stress sensitivity with increasing proppant concentration. The stress sensitivity of rough and smooth fractures decreases with increasing

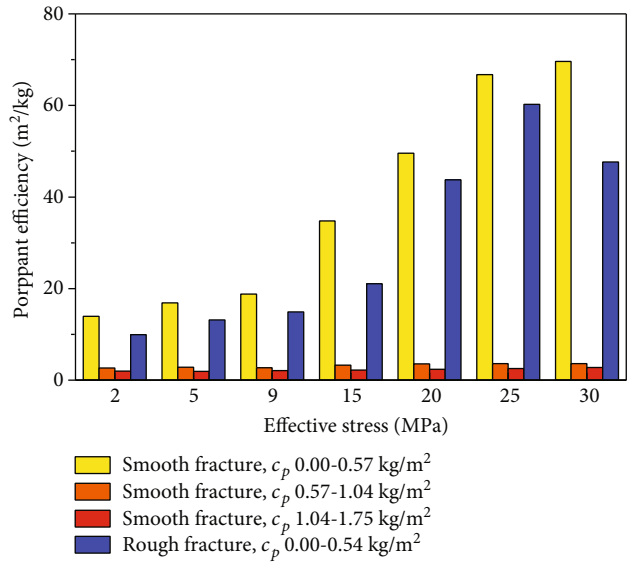

Figure 4: Statistical graph of proppant efficiency.

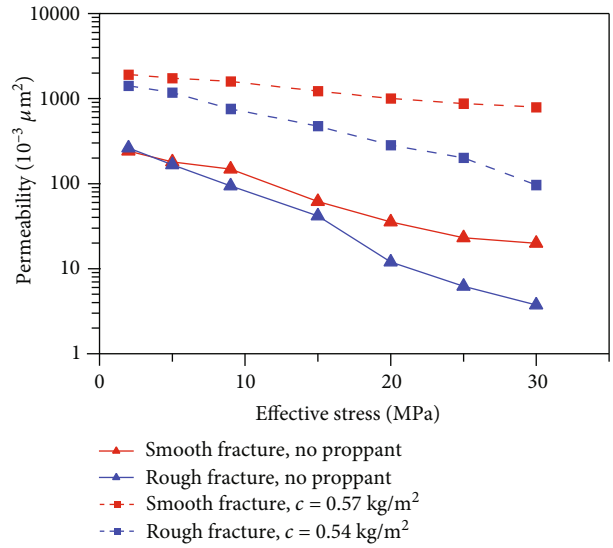

Figure 6: Variation of permeability with effective stress at different fracture surface roughness.

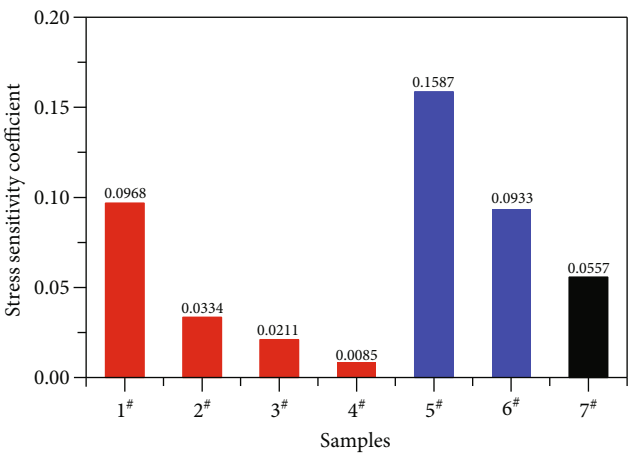

Figure 5: The stress sensitivity coefficient of samples.

proppant concentration. This is because a higher proppant concentration increases its ability to support fractures, making them more difficult to close.

3.3. Effect of Fracture Surface Roughness on Permeability and Stress Sensitivity. Figure 6 shows the variation curve of permeability with effective stress under differing fracture roughness. For cracks without proppant, there is no significant difference in permeability between smooth and rough fractures at low effective stress (≤5 MPa). As the effective stress increases, the permeability of rough fractures decreases more rapidly, and smooth fractures exhibit higher permeability than rough fractures under the same effective stress. It is possible that compared to the smooth fracture, the rough fracture may have a lower fracture closure due to the self-propping effect of rough surfaces under low pressure. Meanwhile, the rough fracture has a long infiltration length due to its high tortuosity. At low pressure, rough fractures are affected by the factors simultaneously, resulting in a permeability similar to smooth fractures. As the effective stress increases, the rough surfaces gradually compact, and the permeability is primarily affected by tortuosity, resulting in a lower permeability than the smooth fractures.

When proppant concentrations are about 0.55 kg/m², smooth fractures have higher permeability than rough fractures. This trend gradually increases with the increase of effective stress. It can be mainly attributed to the nonuniform distribution of proppant and relatively increased fracture surface area caused by the irregular surface of the rough fracture. The nonuniform distribution of proppant leads to more partial fracture closures, resulting in a decrease in overall permeability. The relatively increased surface of the rough fracture causes the proppant concentration to be lower than that of the smooth fracture, resulting in the rough cracks being insufficiently propped, resulting in a lower permeability. For the same reason, rough fracture exhibits higher stress sensitivity than smooth fracture at the same proppant concentration.

4. Fractured Well Productivity for Tight Gas considering Fracture and Matrix Stress Sensitivity

4.1. Derivation of the Fractured Gas Well Productivity Equation. The production of the fractured tight gas well is a coupled matrix and fracture flow process. Therefore, both the matrix and fracture stress sensitivity need to be considered. In addition, considering the fracture's flow resistance, a productivity equation for fractured wells considering fracture and matrix sensitivity is developed based on the formula for the production productivity equation for fractured wells with finite conductivity.

The equivalent well radius of finite conductivity fractures can be calculated as follows [37, 38]:

$$R_{\mathrm{we}} = 2x_f e^{-[3/2+f(C_{FD})]}, \tag{8}$$

where R_{we} is the equivalent well radius, m; x_f is fracture half-length, m; and $f(C_{FD})$ is a function of the dimensionless fracture conductivity, and it can be expressed as follows [39, 40]:

$$f(C_{FD}) = \frac{1.65 - 0.328\mu + 0.116\mu^2}{1 + 0.18\mu + 0.064\mu^2 + 0.005\mu^3}, \tag{9}$$

$$\mu = \ln C_{FD}, \tag{10}$$

$$C_{FD} = \frac{k_f w_f}{k_m x_f}, \tag{11}$$

where C_{FD} is dimensionless fracture conductivity and k_f and k_m are fracture and matrix permeability, respectively, m^2.

The permeability of fracture and matrix considering the stress sensitivity is calculated by

$$k_f = k_{fi} e^{-b_f(p_e - p_w)}, \tag{12}$$

$$k_m = k_{mi} e^{-b_m\left(p_e - \overline{p_m}\right)}, \tag{13}$$

where k_{fi} is initial permeability of fracture, m^2; b_f is the stress sensitivity coefficient of fracture, MPa^{-1}; p_e is original formation pressure, MPa; p_w is bottom hole pressure, MPa; k_{mi} is initial permeability of matrix, m^2; b_m is the stress sensitivity coefficient of matrix, MPa^{-1}; and $\bar{p}_m$ is the average pressure of matrix, MPa. If the calculated fracture permeability is lower than the matrix permeability, the fracture is considered closed, and the fracture permeability is equal to the matrix permeability.

During the gas well production, the reservoir pressure distribution is given by the following equation:

$$\frac{dp}{dr} = \frac{p_e^2 - p_w^2}{\ln R_e/R_{\mathrm{we}}} \frac{1}{2rp}. \tag{14}$$

And the average pressure of the matrix can be calculated by

$$\overline{p_m} = \frac{\int_{R_{\mathrm{we}}}^{R_e} p \cdot 2\pi r dr}{\pi\left(R_e^2 - R_{\mathrm{we}}^2\right)} = \frac{2\int_{R_{\mathrm{we}}}^{R_e} \left(p_e^2 - p_e^2 - p_{\mathrm{we}}^2/\ln R_e/R_{\mathrm{we}} \ln R_e/r\right)^{0.5} r dr}{R_e^2 - R_{\mathrm{we}}^2}. \tag{15}$$

As the average pressure of the matrix is also a function of the equivalent well diameter, the two parameters cannot be calculated directly, so the trial and error method is used instead. The calculation flow chart of equivalent well radius and average matrix pressure is shown in Figure 7. When the relative error ε between the trial and calculated values is less than 5‰, the calculation is stopped, and the two parameters are output.

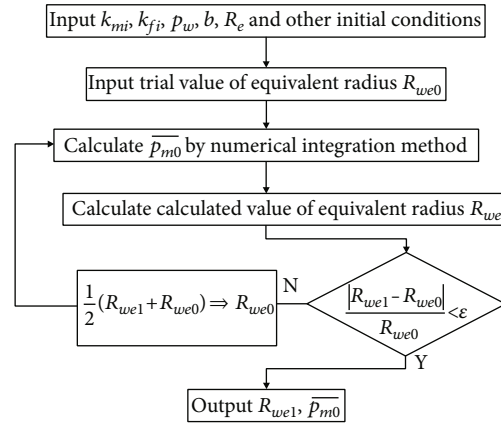

Figure 7: The calculation flow chart of equivalent well radius and matrix average pressure.

The fractured gas well productivity considering fracture and matrix stress sensitivity is

$$Q = \frac{\pi k_m h}{\bar{\mu}\bar{Z}} \frac{Z_{\mathrm{sc}} T_{\mathrm{sc}}}{p_{\mathrm{sc}} T} \frac{p_e^2 - p_w^2}{\ln R_e/R_{\mathrm{we}}}, \tag{16}$$

where $\bar{\mu}$ is average gas viscosity, mPa·s; $\bar{Z}$ is the average gas deviation factor; Z_{sc} is the gas deviation factor in standard condition; T_{sc} is the gas temperature in standard condition, K; p_{sc} is the gas pressure in standard condition, MPa; and T is layer temperature, K.

4.2. Case Study. In the case analysis of this paper, the reservoir parameters are collected from well logging and testing data of the sampled well. The production layer properties of this well are as follows: the overburden pressure is 94.2 MPa, the formation pressure is 40 MPa, the initial permeability is 0.19×10^{-3} $\mu\mathrm{m}^2$, the layer temperature is 120°C, and the reservoir effective thickness is 17.13 m. Based on the assumption that the supply radius is 300 meters, the fracture width is 5 millimeters, and the fracture half-length is 100 meters, the gas well production was calculated at the bottom hole pressure range of 40 to 30 MPa.

Table 3 shows the calculated productivity results of the fractured gas well, where Q is gas well productivity considering stress sensitivity, m^3/d; Q' is gas well productivity without considering stress sensitivity, m^3/d; and η is the productivity loss rate due to stress sensitivity, %. The defining equation is as follows:

$$\eta = \frac{Q' - Q}{Q'} \times 100\%. \tag{17}$$

According to Table 3, stress sensitivity significantly impacts fractured well productivity, and the productivity loss rate due to stress sensitivity increases as bottom hole pressure declines. For unpropped rough fractures, the stress sensitivity can result in a productivity loss of more than 90%. As the bottom hole pressure decreases, the productivity of each fracture tends to increase gradually. Nevertheless, the productivity of unpropped rough fractures ($5^{\#}$) decreases

Table 3: The calculated productivity results of fractured gas well.

Fracture type	Well productivity	p_w (MPa) 40	38	36	34	32	30
	Q	0	2905	5271	7095	8373	9093
$1^{\#}$	Q'	0	6551	12632	18245	23389	28064
	η	—	55.66	58.27	61.11	64.20	67.60
	Q	0	6666	12816	18471	23649	28368
$2^{\#}$	Q'	0	9299	18041	26231	33873	40970
	η	—	28.31	28.96	29.58	30.18	30.76
	Q	0	7747	14945	21609	27754	33395
$3^{\#}$	Q'	0	9683	18819	27410	35460	42972
	η	—	20.00	20.59	21.17	21.73	22.29
	Q	0	9346	18135	26373	34066	41220
$4^{\#}$	Q'	0	10212	19880	29005	37589	45633
	η	—	8.48	8.78	9.07	9.37	9.67
	Q	0	1248	2190	2784	2970	2643
$5^{\#}$	Q'	0	6742	12889	18428	23337	27577
	η	—	81.49	83.01	84.89	87.27	90.42
	Q	0	4239	7962	11173	13876	16070
$6^{\#}$	Q'	0	9009	17326	24951	31881	38112
	η	—	52.94	54.05	55.22	56.48	57.83

when the bottom hole pressure is reduced from 32 MPa to 30 MPa. This is because the infiltration power increased by the reduced bottom hole pressure is less than the resistance caused by stress sensitivity.

Smooth fractures have significantly higher productivity than rough fractures when proppant concentrations are the same. Unpropped smooth fracture is 3.44 times more productive than unpropped rough fracture at 30 MPa, and the value is 1.77 at a proppant concentration of 0.55 kg/m^2. In the same fracture surface roughness, the gas well productivity increases with increasing proppant concentration; especially when the fracture goes from unpropping to propping, the productivity increases the most. At the bottom hole pressure of 30 MPa, the productivity of the unpropped smooth fracture ($1^{\#}$) is 9093 m^3/d. In comparison, the productivity of the smooth fracture ($2^{\#}$) with a proppant concentration of 0.57 kg/m^2 is 28368 m^3/d, a 3.12 times increase in productivity. And for rough fractures, productivity can increase by 6.08 times.

To summarize, during fracturing design, construction, and the subsequent formulation of the flowback strategy, as well as increasing the total proppant addition and increasing the average proppant concentration in the fractures, it will be important to target the fractures that cannot easily be propped, such as secondary fractures and deep parts of main fractures. With a certain proppant amount, the flowback pressure should be controlled, and the timing of flowback should be optimized to reduce the proppant backflow to improve the overall proppant concentration in the fracture. During hydraulic fracturing, the construction process can be optimized by the sand slug addition method to make the proppant enter the deep part of the fracture as much as possible, and the proppant can be distributed more equally.

5. Conclusions

In this paper, the effects of proppant concentration and fracture surface roughness on permeability and stress sensitivity are investigated experimentally. The productivity equation of fractured gas well is derived to study the effect of stress sensitivity on productivity. The main conclusions are obtained as follows:

(1) The proppant can effectively enhance permeability and reduce the stress sensitivity of artificial fracture. As proppant concentration increases, the fracture permeability increases, the fracture stress sensitivity decreases, and the proppant efficiency decreases. For the same increment in proppant concentration, the artificial fracture has the most significant enhancement in permeability from unpropped to propped

(2) The roughness of the fracture surface can significantly affect fracture permeability and stress sensitivity. For unpropped fractures, the permeability of smooth fracture and rough fracture is similar under

low effective stress (≤5 MPa). For unpropped fractures under high effective stress (≥10 MPa) and propped fractures, the rough fractures have lower permeability and higher stress sensitivity than smooth fractures

(3) The stress sensitivity dramatically impacts the productivity of fractured wells. Under the same proppant concentration, the stress sensitivity is lower, and the gas production is higher for smooth fractures. As proppant concentration increases, fracture permeability increases, stress sensitivity decreases, and gas well productivity increases. The most significant increase in fractured well productivity occurs when the artificial fracture changes from no proppant to proppant. During hydraulic fracturing, reasonable measures should be taken to distribute the proppant uniformly and to enhance the effective propping of the deep parts of the fractures

Data Availability

The figures and tables used to support the findings of this study are included in the article.

Conflicts of Interest

The authors declare that there is no conflict of interest regarding the publication of this paper.

Acknowledgments

The authors would like to sincerely thank those techniques which have contributed to this research.

References

[1] W. H. Haider, "IPTC-19729-MS estimates of total oil & gas reserves in the world, future of oil and gas companies and smart investments by E & P companies in renewable energy sources for future energy needs," in *International Petroleum Technology Conference*, Dhahran, Saudi Arabia, 2020.

[2] W. Hu, J. Bao, and B. Hu, "Trend and progress in global oil and gas exploration," *Petroleum Exploration and Development*, vol. 40, no. 4, pp. 439–443, 2013.

[3] L. Zheng, P. Wei, Z. Zhang et al., "Joint exploration and development: a self-salvation road to sustainable development of unconventional oil and gas resources," *Natural Gas Industry B*, vol. 4, no. 6, pp. 477–490, 2017.

[4] C. Jia, M. Zheng, and Y. Zhang, "Unconventional hydrocarbon resources in China and the prospect of exploration and development," *Petroleum Exploration and Development*, vol. 39, no. 2, pp. 139–146, 2012.

[5] Z. Yang and C. Zou, ""Exploring petroleum inside source kitchen": connotation and prospects of source rock oil and gas," *Petroleum Exploration and Development*, vol. 46, no. 1, pp. 181–193, 2019.

[6] H. Cheng, J. Wei, and Z. Cheng, "Study on sedimentary facies and reservoir characteristics of Paleogene sandstone in Yingmaili block, Tarim Basin," *Geofluids*, vol. 2022, Article ID 1445395, 14 pages, 2022.

[7] J. Han, H. Cheng, Y. Shi, L. Wang, Y. Song, and W. Zhnag, "Connectivity analysis and application of fracture cave carbonate reservoir in Tazhong," *Science Technology and Engineering*, vol. 16, no. 5, pp. 147–152, 2016.

[8] T. Guo, S. Zhang, Z. Qu, T. Zhou, Y. Xiao, and J. Gao, "Experimental study of hydraulic fracturing for shale by stimulated reservoir volume," *Fuel*, vol. 128, pp. 373–380, 2014.

[9] C. Zou, D. Dong, S. Wang et al., "Geological characteristics and resource potential of shale gas in China," *Petroleum Exploration and Development*, vol. 37, no. 6, pp. 641–653, 2010.

[10] L. Wuguang, B. Zhong, X. Zhang, Z. Hu, and L. Xie, "Evaluating method of the stress sensitivity for the artificial fracture in the shale," *Petroleum Geology & Oilfield Development in Daqing*, vol. 35, no. 3, pp. 159–164, 2016.

[11] Z. Zhang, S. He, G. Liu, X. Guo, and S. Mo, "Pressure buildup behavior of vertically fractured wells with stress-sensitive conductivity," *Journal of Petroleum Science and Engineering*, vol. 122, pp. 48–55, 2014.

[12] A. Reinicke, E. Rybacki, S. Stanchits, E. Huenges, and G. Dresen, "Hydraulic fracturing stimulation techniques and formation damage mechanisms– implications from laboratory testing of tight sandstone-proppant systems," *Chemie der Erde-Geochemistry-Interdisciplinary Journal for Chemical Problems of the Geosciences and Geoecology*, vol. 70, pp. 107–117, 2010.

[13] V. S. Pathi, *Factors affecting the permeability of gas shales*, PhD diss., University of British Columbia, 1995.

[14] G. R. L. Chalmers, D. J. K. Ross, and R. M. Bustin, "Geological controls on matrix permeability of Devonian Gas Shales in the Horn River and Liard basins, northeastern British Columbia, Canada," *International Journal of Coal Geology*, vol. 103, pp. 120–131, 2012.

[15] H. Yuanzhi and W. Enzhi, "Experimental study on coefficient of sensitiveness between percolation rate and effective pressure for low permeability rock," *Chinese Journal of Rock Mechanics and Engineering*, vol. 26, no. 2, pp. 410–414, 2007.

[16] Q. Lei, W. Xiong, C. Yuan, and Y. S. Wu, *Analysis of Stress Sensitivity and Its Influence on Oil Production from Tight Reservoirs - eScholarship*, Society of Petroleum Engineers, 2008.

[17] R. Zhang, Z. Ning, F. Yang, H. Zhao, and Q. Wang, "A laboratory study of the porosity-permeability relationships of shale and sandstone under effective stress," *International Journal of Rock Mechanics and Mining Sciences*, vol. 81, pp. 19–27, 2016.

[18] R. Zhang, *Effective stress law and stress dependent mechanism for the permeability of shale*, Doctoral thesis. China University of Petroleum, 2018.

[19] M. M. Rahman and S. S. Rahman, "Fully coupled finite-element–based numerical model for investigation of interaction between an induced and a preexisting fracture in naturally fractured poroelastic reservoirs: fracture diversion, arrest, and breakout," *International Journal of Geomechanics*, vol. 13, no. 4, pp. 390–401, 2013.

[20] J.-C. Sun, Y. Zheng-Ming, W. Guo-Qi, and Z. Xue-Min, "Characterization of stress-dependent permeability of volcanic gas reservoir of different types of pore structure," *Rock and Soil Mechanics*, vol. 33, 2012.

[21] Z. Liu, J. Zhao, P. Kang, and J. Zhang, "*An experimental study on simulation of stress sensitivity to production of volcanic gas from its reservoir*," *Journal of the Geological Society of India*, vol. 86, no. 4, pp. 475–481, 2015.

[22] J. J. Dong, J. Y. Hsu, W. J. Wu et al., "Stress-dependence of the permeability and porosity of sandstone and shale from TCDP Hole-A," *International Journal of Rock Mechanics & Mining Sciences*, vol. 47, no. 7, pp. 1141–1157, 2010.

[23] K. Xiao, Z. Zhang, R. Zhang et al., "Anisotropy of the effective porosity and stress sensitivity of coal permeability considering natural fractures," *Energy Reports*, vol. 7, pp. 3898–3910, 2021.

[24] D. Yang, W. Wang, K. Li, W. Chen, J. Yang, and S. Wang, "Experimental investigation on the stress sensitivity of permeability in naturally fractured shale," *Environment and Earth Science*, vol. 78, no. 2, 2019.

[25] T. Hou, S. Zhang, X. Ma et al., "Experimental and theoretical study of fracture conductivity with heterogeneous proppant placement," *Journal of Natural Gas Science and Engineering*, vol. 37, pp. 449–461, 2017.

[26] M. Fan, Y. Han, J. McClure, and C. Chen, "Hydraulic fracture conductivity as a function of proppant concentration under various effective stresses: from partial monolayer to multilayer proppants," in *SPE/AAPG/SEG Unconventional Resources Technology Conference*, Austin, Texas, USA, 2017.

[27] Y. Zhang, H. Ge, G. Liu et al., "Experimental study of fracturing fluid retention in rough fractures," *Geofluids*, vol. 2019, Article ID 2603296, 20 pages, 2019.

[28] J. Wang, Y. Huang, F. Zhou, and X. Liang, "The influence of proppant breakage, embedding, and particle migration on fracture conductivity," *Journal of Petroleum Science and Engineering*, vol. 193, p. 107385, 2020.

[29] R. Shaibu, B. Guo, P. B. Wortman, and J. Lee, "Stress-sensitivity of fracture conductivity of Tuscaloosa Marine Shale cores," *Journal of Petroleum Science and Engineering*, vol. 210, article 110042, 2022.

[30] L. Dong, D. Wang, F. Li, X. Fu, and M. Wang, "Investigation of fracture width change under closure pressure in unconventional reservoir based on the Hertz contact theory," *Geofluids*, vol. 2021, Article ID 1268352, 6 pages, 2021.

[31] G. Lei, S. Gu, L. Dong, Q. Liao, and L. Xue, "Particle plugging in porous media under stress dependence by Monte Carlo simulations," *Journal of Petroleum Science and Engineering*, vol. 207, article 109144, 2021.

[32] H. Chen, T. Zhou, H. Fan, J. Zhang, and S. Yang, "Preparation method and stress sensitivity of core samples with hydraulic fractures in shale reservoirs," *Acta Petrolei Sinica*, vol. 41, no. 9, p. 1117, 2020.

[33] N. Bo, X. Zuping, L. Xianshan et al., "Production prediction method of horizontal wells in tight gas reservoirs considering threshold pressure gradient and stress sensitivity," *Journal of Petroleum Science and Engineering*, vol. 187, article 106750, 2020.

[34] L. Jiang, J. Liu, T. Liu, and D. Yang, "Semi-analytical modeling of transient pressure behaviour for a fractured vertical well with hydraulic/natural fracture networks by considering stress- sensitive effect," *Journal of Natural Gas Science and Engineering*, vol. 82, article 103477, 2020.

[35] X. Xinli, "Stress sensitivity of low-permeability reservoir contain- ing micro-fracture and its influence on productivity," *Special Oil & Gas Reservoirs*, vol. 22, no. 1, p. 4, 2015.

[36] R. Liu, H. Liu, H. Zhang, Y. Tao, and M. Li, "Study of stress sensitivity and its influence on oil development in low permeability reservoir," *Chinese Journal of Rock Mechanics & Engineering*, vol. 30, pp. 2697–2702, 2011.

[37] F. Zhang, S. Zhao, J. Qin, Y. Deng, W. Sun, and J. Yi, "Productivity of the horizontal well with finite-conductivity fractures," *Natural Gas Geoscience*, vol. 20, no. 5, 2009.

[38] B. Meyer, R. Jacot, and A. Inc, *SPE 95941 Pseudosteady-State Analysis of Finite-Conductivity Vertical Fractures Presented an Approximate Analytical Mathematical Model for Predicting the Productivity Ratio Increase of Finite-Conductivity Fractures in Pseudosteady*, 2005.

[39] M. Economides, R. Oligney, and P. Valkó, *Unified Fracture Design: Bridging the Gap between Theory and Practice*, Orsa Press, 2002.

[40] M. K. Rahman, M. M. Rahman, and A. H. Joarder, "Analytical production modeling for hydraulically fractured gas reservoirs," *Petroleum Science and Technology*, vol. 25, no. 6, pp. 683–704, 2007.